Biocatalysis and Biotransformation

ISSN: (Print) (Online) Journal homepage: https://www.tandfonline.com/loi/ibab20

A new peroxidase from the roots of the Algerian white turnip (*Brassica rapa*, variety *rapa*): extraction, purification, characterisation, and antioxidant potential

Amel Dahdouh, Nawel Boucherba, Khelifa Bouacem, Sondes Mechri, Adel Amirouche, Ali Aksas, Bassem Jaouadi & Djamel Edine Kati

To cite this article: Amel Dahdouh, Nawel Boucherba, Khelifa Bouacem, Sondes Mechri, Adel Amirouche, Ali Aksas, Bassem Jaouadi & Djamel Edine Kati (2022) A new peroxidase from the roots of the Algerian white turnip (*Brassica rapa*, variety *rapa*): extraction, purification, characterisation, and antioxidant potential, Biocatalysis and Biotransformation, 40:6, 432-449, DOI: 10.1080/10242422.2021.1953485

To link to this article: https://doi.org/10.1080/10242422.2021.1953485

Published online: 19 Jul 2021.

BIOCATALYSIS AND BIOTRANSFORMATION
2022, VOL. 40, NO. 6, 432–449
https://doi.org/10.1080/10242422.2021.1953485

Taylor & Francis
Taylor & Francis Group

RESEARCH ARTICLE

A new peroxidase from the roots of the Algerian white turnip (*Brassica rapa*, variety *rapa*): extraction, purification, characterisation, and antioxidant potential

Amel Dahdouh[a], Nawel Boucherba[b], Khelifa Bouacem[c], Sondes Mechri[d], Adel Amirouche[a], Ali Aksas[e], Bassem Jaouadi[d]* and Djamel Edine Kati[a]*

[a]Laboratoire de Biochimie Appliquée (LBA), Faculté des Sciences de la Nature et de la Vie (FSNV), Université de Bejaia, Bejaia, Algeria; [b]Laboratoire de Microbiologie Appliquée (LMA), Faculté des Sciences de la Nature et de la Vie (FSNV), Université de Bejaia, Bejaia, Algeria; [c]Laboratoire de Biologie Cellulaire et Moléculaire (LBCM), Equipe de Microbiologie, Faculté des Sciences Biologiques (FSB), Université des Sciences et de la Technologie Houari Boumediene (USTHB), Alger, Algeria; [d]Laboratoire de Biotechnologie Microbienne, Enzymatique et de Biomolécules (LBMEB), Centre de Biotechnologie de Sfax (CBS), Université de Sfax, Sfax, Tunisia; [e]Laboratoire de Biotechnologies Végétales et Ethnobotanique (LBVE), Faculté des Sciences de la Nature et de la Vie (FSNV), Université de Bejaia, Bejaia, Algeria

ABSTRACT

Due to its various biological activities, the roots of *Brassica rapa* (turnip), has been applied as a therapeutic agent in traditional medicine. The current study aimed to purify a plant peroxidase (POD; designated as TRP) from Algerian white turnip (*B. rapa*, variety *rapa*) roots, to homogeneity and to characterise it biochemically. The molecular weight of the purified TRP was determined to be ~58 kDa as estimated by sodium dodecyl sulphate polyacrylamide gel electrophoresis (SDS-PAGE) and high-performance liquid chromatography (HPLC). The TRP Reinheitzahl values (RZ) and specific activity were 2.9 and 14,500 U/mg, respectively. Its N-terminal sequence exhibited high identity with those of class III-PODs. TRP showed optimal activity at 55 °C and pH 6 (guaiacol), was completely inhibited by sodium azide (NaN_3) and potassium cyanide (KCN) and exhibited greater catalytic efficiency than that of the well-known horseradish peroxidase (HRP) from *Armoracia rusticana*. TRP demonstrated antioxidant activities with 45% and 61.49% of 2,2′-azino-bis(3-ethylbenzothiazoline-6-sulfonic acid) ($ABTS^{\bullet}$) and hydroxyl ($^{\bullet}OH$) radical scavenging, respectively, as well as ferrous ion chelating (52.96%) and reducing (48.32%) powers. This study provides information regarding the potential role of TRP in enzyme therapy (as applied in the pharmaceutical and medicinal industries), with biological eradication of free radicals.

Abbreviations: BHT: butylated hydroxytoluene; CFU: colony forming unit; DTNB: 5,5-dithio-bis-2-nitrobenzoic acid; HRP: horseradish peroxidase; HR: high resolution; H_2O_2: hydrogen peroxide; PhO: phenol oxidase; PVPP: polyvinylpolypyrrolidone; PODs: plant peroxidases; Rt: retention time; ROS: reactive oxygen species; RZ: Reinheitzahl value; TRP: turnip roots peroxidase.

ARTICLE HISTORY
Received 26 January 2021
Revised 5 June 2021
Accepted 4 July 2021

KEYWORDS
White turnip; plant peroxidase; antioxidant properties; hydroxyl radical scavenging; ferrous ion chelation; reducing powers

1. Introduction

Our need to coexist with Nature is highlighted by the range of natural products currently being sourced from plants, animals, and minerals for the treatment of human illnesses (Wedelsbäck Bladh and Olsson 2011; Zourgui et al. 2020; Lataief et al. 2021). Medicinal plants are currently in great demand and their use and application is escalating. This is mainly due to the belief that products derived from medicinal plants exhibit great health benefits (Wedelsbäck Bladh and Olsson 2011; Zourgui et al. 2020; Lataief et al. 2021). This can be seen in the celebrated centuries-old, traditional Tibetan medicine practices, where the turnip, belonging to the *Brassica* subspecies of the family *Cruciferae*, has found a wide range of applications, including anti-hypoxia, detoxification, and heat-clearing (Wedelsbäck Bladh and Olsson 2011; Hua et al. 2013). Recent evidence-based studies have shown that the fleshy roots of turnips are rich in dietary fibre, folic acid, vitamins A, C, E, and B_6, copper, and calcium. In addition to being a type of vegetable, turnips are also used as a key source of peroxydolytic enzymes. Classified as oxidoreductases, peroxidases

CONTACT Nawel Boucherba boucherbanawel@yahoo.fr Laboratoire de Microbiologie Appliquée (LMA), Faculté des Sciences de la Nature et de la Vie (FSNV), Université de Bejaia, Bejaia, Algeria; Bassem Jaouadi bassem.jaouadi@cbs.rnrt.tn Laboratoire de Biotechnologie Microbienne, Enzymatique et de Biomolécules (LBMEB), Centre de Biotechnologie de Sfax (CBS), Université de Sfax, Sfax, Tunisia
#The last two authors have contributed equally to the supervision of this study.

are responsible for the exchange of electrons from a natural substrate (donor) to another synthetic compound (acceptor) (Dahdouh et al. 2020). They are haem-containing proteins that may contribute to diminish hydrogen peroxide (H_2O_2), while oxidising a second substrate. Due to these oxidoreduction reactions, these enzymes are among the key antioxidant biocatalysts that play a main role in detoxification and oxidative stress relief of reactive oxygen species (ROS) (Wedelsbäck Bladh and Olsson 2011; Hua et al. 2013). They oxidise a diverse set of organic and inorganic compounds by reducing H_2O_2 and catalysing the 1- or 2-electron oxidation of a wide range of substrates (Al Ghouleh et al. 2011). Non-animal peroxidases are classified into three classes: Class I peroxidases are known to be present in bacteria and fungi, and include cytochrome C peroxidase, ascorbate peroxidase, and catalase; class II peroxidases is known to be present in fungi and actinobacteria and include extracellular fungal manganese and lignin-degrading peroxidases; and class III peroxidases are present only in higher plants. Peroxydolytic enzymes are distinct forms of isoenzymes that can oxidise a wide range of phenolic substrates such as catechin, catechol, chlorogenic acid, guaiacol, and pyrogallol. Various studies focussed on peroxidases sourced from plants have been reported (Maciel et al. 2007): manioc or cassava (*Manihot utilissima*), peach (*Prunus persica*), horseradish (*Armoracia rusticana*), globe or green artichoke (*Cynara scolymus L.*), yam or giant taro (*Alocasia macrorhiza*), sweet potato (*Ipomoea batatas* ex L., Lam.), zucchini or courgette (*Cucurbita pepo*), turnip or white turnip (*Brassica campestre rapifera*), and others (Sumathi and Pattabiraman 1977; Dirlewanger et al. 2002; Freitas et al. 2004; Lavery et al. 2010).

The well-known horseradish peroxidase (HRP) extracted from *Armoracia rusticana* roots is a good example of a plant-derived peroxidase with great biotechnological and commercial benefits (Lavery et al. 2010; Ambatkar and Mukundan 2014). In microbial biotechnology and enzyme engineering fields, peroxidases from plants (PODs) are of keen interest. Firstly, the extraction of enzymes from plant sources is inexpensive and less complicated than its production from a microbial source. Secondly, PODs are applied for many purposes in biotechnological applications, not only in the decolorisation of dyes, biodegradation of pigments from wastewater, and the removal of recalcitrant aromatic compounds from drinking water, but also in pharmaceutical and medicinal approaches to explore their antioxidant potential. PODs are largely used in preparation of medical diagnostic kits, as markers for ROS in food processes and as a catalyst in the synthesis of phenolic resins for commercial purposes (Falade et al. 2017; Khanmohammadi et al. 2018). In addition, the structure-function relationships of peroxidases are central to understanding both cells and organisms. Beyond this, there are a number of important reasons for purifying peroxidases (Serrano-Martínez et al. 2008). Once a peroxidase is purified, it is possible to study its enzymology, understand its affinity for particular substrates, and/or analyse its ability to catalyse enzymatic reactions. Such approaches have allowed us to understand how peroxidases can act as biocatalysts. The availability of purified proteins allows modifying specific residues to help understand how these residues confer particular structures or allow the peroxidase to operate as a catalyst (Serrano-Martínez et al. 2008; Fortea et al. 2011). Moreover, the understanding of how particular amino-acid residues are involved in peroxidase function, especially when it is combined with knowledge of the 3 D structure of the peroxidase HRP, helps us to understand how particular sequences in peroxidase are involved in biological functions. The accumulation of this type of knowledge derived from the study of peroxidases, combined with a tremendous amount of information in DNA databases have allowed a construction of up-to-date peroxidase databases (PeroxiBases) such as: https://www.uniprot.org/database/DB-0072; https://peroxibase.toulouse.inra.fr/; http://peroxibase.isb-sib.ch; and https://bio.tools/peroxibase.

In a previous study and using response surface methodology, the authors described the optimisation of peroxidase activity from Algerian white turnip fresh roots, *B. rapa*, variety *rapa* (Dahdouh et al. 2020), and the optimisation of the immobilisation of this crude peroxidase using microencapsulation by double emulsion in polylactic acid polymer (Dahdouh et al. 2021). The aim of the current study is twofold. First, we provide a detailed description of the isolation and purification methods of a new peroxidase from the roots of Algerian white turnip. Second, we report the biochemical characterisation of this peroxidase (designated as TRP). The present investigation provides information regarding the antioxidant potential of the TRP as potential enzyme therapy applied in the pharmaceutical, cosmetic, and medicinal industries.

2. Materials and methods

2.1. Materials

The roots of *B. rapa*, variety *rapa* were harvested throughout the year (Bejaia, Algeria). The roots were

collected and transported to the laboratory, thoroughly washed with distilled water, and cut into small pieces (Dahdouh et al. 2020, 2021). The latter were used for the extraction, characterisation, and antioxidant assessment of peroxidase activity. The roots were used fresh or stored at 4 °C for up to one week. The extract was used immediately for the assessment of peroxidase activity or stored at −20 °C for up to three months.

The 2-methoxyphenol (guaiacol), 1,2,3-trihydroxybenzene (pyrogallol), 1,2-dihydroxybenzene (catechol), methoxybenzene (anisole), bovine serum albumin (BSA), ABTS, HRP (a well-known commercial enzyme), and polyvinylpolypyrrolidone (PVPP) were supplied by the Sigma-Aldrich Corporation (St. Louis, MO, USA). Bradford-based assay and Coomassie brilliant blue R250 were obtained from Bio-Rad Laboratories Inc. (Hercules, CA, USA). The protein marker and chromatography supports used for peroxidase purification are as follow: low molecular weight (LMW) protein marker supplied by Amersham Pharmacia Biotech Inc. (Piscataway, NJ, USA), manually prepared Sephacryl® S-200 HR (high resolution) (2.5 cm ID × 150 cm bed length) and Mono Q-Sepharose® (2.6 cm ID × 50 cm bed length) columns were prepared in columns bought from Cytiva (Björkgatan, Uppsala, Sweden), and the analytical silica-based pre-packed Shodex Protein® WK-802.5 HPLC column (8 mm ID × 300 mm bed length) was obtained from Showa Denko K.K. (SDK, Kawasaki, Japan). The UV-VIS spectrophotometer was obtained from Shimadzu UV-2700 (Nakagyō-Ku, Kyoto, Japan). The protein analyser using a gas-phase protein sequencer system (Model 473 A, ABI) was obtained from Applied Biosystems (Foster City, CA, USA).

The buffers used were Buffer A: 50 mM 2-(*N*-morpholino)ethanesulfonic acid (MES) buffer supplemented with 2 mM $MnSO_4$ (pH 6); Buffer B: 50 mM 4-(2-hydroxyethyl)-1-piperazineethanesulfonic acid) (HEPES) buffer supplemented with 25 mM NaCl (pH 6.4); Buffer C: 25 mM 3-(*N*-morpholino)propanesulfonic acid (MOPS) buffer (pH 7.1); Buffer D: 100 mM phosphate buffer (pH 6.5) supplemented with 1% (*w*/*v*) PVPP and 2 mL/g of roots; Buffer E: 200 mM sodium phosphate buffer (pH 6.6); and Buffer F: 50 mM phosphate buffer (pH 7.4).

2.2. Peroxidase assay

All assays were performed in 1-mL volumes at 25 °C in a UV/VIS spectrophotometer (Shimadzu UV-2700 Kyoto, Japan). Increases in absorbance were recorded at selected wavelengths depending on the substrate used. The peroxidase activity was determined spectrophotometrically at 470 nm ($A_{470\,nm}$) when using guaiacol as the hydrogen donor and monitoring tetraguaiacol formation as described by Rojas-Reyes et al. (2014). The assay mixture contained 250 µL of 45 mM guaiacol dissolved in the buffer A, 250 µL of 25 mM 4-aminoantipyrine, 250 µL of 0.5 mM H_2O_2, and 250 µL of suitably diluted enzyme solution.

The peroxidase activity was calculated as follows:

$$A = [(\Delta Abs/\Delta t) \times V_{tot} \times f]/[V_{enz} \times \varepsilon \times l], \qquad (1)$$

where A is the peroxidase activity (in U/mL), $\Delta Abs/\Delta t$ is the slope of absorption intensity versus time (in minutes), V_{tot} is the total reaction volume (mL), f is the dilution factor, V_{enz} is the volume of enzyme used (mL), ε is the extinction coefficient, and l is the path length of the cell. Here a guaiacol extinction coefficient of 26.6 $mM^{-1}\,cm^{-1}$ was used and the light path length of the cell was 1 cm. The concentration of the active enzyme in the assay is proportional to the rate of H_2O_2 consumption. The assay was initiated with the addition of freshly prepared H_2O_2, and the increase in absorbance ($A_{470\,nm}$) was recorded every 30 s for 5 min at 25 °C and pH 6. One unit of the peroxidase activity is defined as the amount of substrate (µmole) consumed per minute under the standard assay conditions described here.

2.3. Purification of the turnip roots peroxidase (TRP)

The white turnip roots contain elevated amounts of polyphenols and nucleotides, that lead to the brown colour of the crude extract throughout the extraction procedure of the peroxidase, which were eradicated by the addition of 1% (*w*/*v*) insoluble PVPP and treatment with polyethylene amine (Rosa et al. 2020). The entire procedure was performed at 4 °C except where otherwise indicated, and all centrifugation steps were performed at 9000×*g* for 30 min.

2.3.1. Crude extract preparation

About 200 g of fresh Algerian white turnip roots (*B. rapa*, variety *rapa*) were homogenised in buffer D at 4 °C, in a commercial blender from Groupe SEB Moulinex (Ecully, Lyon, France) until no lumps were observed. To eliminate the suspended fibrous solid part, the homogenate obtained was filtered through cotton wool, and centrifuged as stated by Rosa et al. (2020). The obtained supernatant was used as the crude peroxidase solution.

2.3.2. Ammonium sulphate fractionation

About 400 mL of the crude enzyme extract containing 950,000 total units of peroxidase, was differentially fractionated with ammonium sulphate salt $(NH_4)_2SO_4$ (Wingfield 2001). The salt was added to the extract with steady stirring overnight (on ice) for complete protein precipitation. The crude extract was brought to 30% saturation (176 g/L). After 1 h, the precipitate was removed and the clear supernatant solution brought to 80% saturation (351 g/L). The precipitate was resuspended in buffer B and the insoluble material removed. Collected fractions with selected precipitation (30%-80%) saturation were measured for peroxidase activity (U/mL) and protein concentration (mg/mL), and the enzyme specific activity (U/mg) calculated.

2.3.3. Gel-filtration chromatography

The clear supernatant (30 mL) was injected into a Sephacryl® S-200 HR column which was equilibrated with buffer B. Peroxidase elution was carried out with buffer B at a rate of 1 mL/min. The fractions exhibiting peroxidase activity were pooled and used for the determination of protein concentration and enzyme activity.

2.3.4. Anion exchange chromatography

The pooled active fractions from the Sephacryl® S-200 HR column were applied to a Mono Q-Sepharose® anion exchanger previously equilibrated with buffer C. The column was washed with buffer C until the effluent absorbance at 280 nm ($A_{280\,nm}$) was zero. No peroxidase activity was noticed in the rinsed flow. The adsorbed material was eluted with a linear NaCl gradient of 0 mM to 500 mM (650 mL) in buffer C at a rate of 0.5 mL/min. Fractions collected were evaluated for the presence of protein (by measuring absorbance at $A_{280\,nm}$) and by measuring the peroxidase activity at $A_{470\,nm}$. The pooled fractions with TRP activity were concentrated with centrifugal micro-concentrators (Amicon Inc., Beverly, MA, USA) with 30 kDa cut-off membranes and were stored at −20 °C in a 20% glycerol (*v*/*v*) solution and then used for the characterisation of the peroxidase.

2.4. Protein concentration determination

Protein concentration of the samples obtained during the different purification steps was determined according to the method of Bradford (1976) using the Dc protein assay kit from Bio-Rad Laboratories (Inc., Hercules, CA, USA) with BSA as a reference. The absorbance was determined at 595 nm ($A_{595\,nm}$).

2.5. Analytical methods

The subunit molecular weight of the purified TRP enzyme from Algerian white turnip roots (*B. rapa*, variety *rapa*) was determined by SDS-PAGE under denaturing conditions (Laemmli 1970) using the Mini-PROTEAN® system from Bio-Rad Laboratories, Inc. (Hercules, CA, USA). Protein bands were visualised with Bio-Safe™ Coomassie Brilliant Blue G-250 staining (Bio-Rad Laboratories, Inc., Hercules, CA, USA). Under native conditions, the molecular weight of TRP was resolved in comparison to the standard LMW protein marker and confirmed by gel-filtration chromatography using a Shodex Protein® WK-802.5 HPLC column, equilibrated with buffer C (Allala et al. 2019). Zymography analysis of peroxidase activity was achieved by incubating the SDS-PAGE gels in a mixture containing 28 mL of buffer A, 1 mL of 200 mM guaiacol, and 1 mL of 500 mM H_2O_2 for 30 min. The stained SDS-PAGE gels were rinsed with water. The bands representing the purified TRP enzyme were separated in the SDS-PAGE gels, and electro-transferred to a polyvinylidene difluoride (PVDF) blotting membrane and its N-terminal sequence was identified by the automated Edman degradation procedure using an Applied Biosystem Model 473 A gas-phase sequencer (Applied Biosystems, CA, USA).

2.6. Spectral and physico-chemical characterisation of the purified TRP

2.6.1. Spectral analysis

The absorption spectrum (from 200 nm to700 nm) of the purified TRP was spectrophotometrically recorded at 25 °C. The proto-haem content was determined by the pyridine ferro-haemochrome protocol as described by Yumoto et al. (2000). The haem content was measured based on the extinction coefficient (ε) of the pyridine haemochrome b as 34.5 $mM^{-1}\,cm^{-1}$.

2.6.2. Effect of guaiacol, H_2O_2, and 4-aminoantipyrine concentration on reaction rate

The effect of different concentrations of guaiacol on enzyme activity was evaluated from 1 mM to 100 mM. The effect of H_2O_2 concentration on the purified TRP activity was calculated at different concentrations as reported by Jaouadi et al. (2014). The effect of 4-aminoantipyrine concentration on the reaction rate was also measured from 1 mM to 40 mM. The peroxidase

activity was measured under the standard conditions (as described above).

2.6.3. Evaluation of the effect of selected inhibitors and metal ions on TRP stability

The effect of selected haem-protein inhibitors and specific reagents were studied. NaN_3, KCN, L-cysteine, hydroxylamine, 5,5-dithio-bis-2-nitrobenzoic acid (DTNB), *N*-ethylmaleimide (NEM), iodoacetamide, SDS, β-mercaptoethanol (β-ME), and DL-dithiothreitol (DL-DTT) were tested at different concentrations. The effects of various metal ions (Mn^{2+}, Mg^{2+}, Ca^{2+}, Cu^{2+}, Ba^{2+}, Fe^{2+}, Zn^{2+}, Co^{2+}, Ni^{2+}, Cd^{2+}, and Hg^{2+}) on enzyme activity were also investigated at a concentration of 2 mM. The residual peroxidase activity was calculated after the incubation of TRP enzyme with each inhibitor or metal ion for 1 h at 55 °C and compared to the control assay.

2.6.4. Effect of different pH on TRP activity and stability

The purified TRP activity was monitored at 55 °C at different pH (2–11) using guaiacol as the substrate. The pH stability of the peroxidase was ascertained by incubating the TRP in different buffer solutions from pH 4–8 at 30 °C for 12 h. Aliquots were collected periodically, and residual peroxidase activity was determined under the optimum assay conditions. The buffer systems, supplemented with 2 mM $MnSO_4$, were all prepared at 50 mM (Jaouadi et al. 2014).

2.6.5. Effect of different temperatures on TRP activity and stability

The effect of different temperatures on the TRP activity was determined at 30–80 °C and pH 6, for 5 min using guaiacol. The thermo-stability of the peroxidase was determined by incubating the enzyme for 12 h with and without 2 mM $MnSO_4$, at 40 °C, 50 °C, and 60 °C, pH 6. As described previously, the untreated TRP was used as a control and taken as 100% (Rekik et al. 2019).

2.7. Kinetic study

The kinetic parameters [Michaelis–Menten constant (K_m), maximal reaction velocity (V_{max}), catalytic constant or the turnover number (k_{cat}), and catalytic efficiency (k_{cat}/K_m)] of the purified TRP and HRP were assessed based on their initial activity rates by Lineweaver–Burk plots, using guaiacol, pyrogallol, catechol, and anisole as phenolic substrates. The temperature and pH values used in the kinetic study were determined under the optimum enzymatic conditions for each peroxidase (TRP at 55 °C and pH 6 and HRP at 40 °C and pH 7). The enzymatic reaction was performed for 2 min at different substrate concentrations [1 mM–100 mM], in assay buffer with constant enzyme concentrations (10 µg/mL), and at a final volume of 1 mL. The initial velocities were measured on the linear section of the kinetics plots and the apparent K_m and V_{max} were calculated from a hyperbolic regression analysis using the software Hyper32 version 1.0.0.

2.8. Antioxidant activity of the turnip enzymatic extract

2.8.1. ABTS radical scavenging

The potential of peroxidase activity to eradicate free radicals was determined with the ABTS free-radical staining as reported elsewhere (Sellem et al. 2016; Mechri et al. 2020a). Briefly, the ABTS mono-cation radicals were produced by reacting a 7 mM ABTS solution with $K_2S_2O_8$ (2.45 mM). The reaction mixture was diluted with ethanol to attain an absorbance of 0.7 at 734 nm ($A_{734\,nm}$). 20 µL of each extract, or butylated hydroxytoluene (BHT), also known as dibutylhydroxytoluene, at different concentrations were added to 180 µL of ABTS·+. The percentage of the ABTS·+ scavenging activity was measured by determining the reduction in absorbance at different concentrations as follows:

$$Antioxidantactivity(\%) = [(A_c - A_t)/\mathrm{A_c})] \times 100, \quad (2)$$

where A_c and A_t indicating the absorbance of the standard and the sample, respectively.

2.8.2. Ferrous ion chelating power

Different concentrations of extracts were added to 100 µL of 0.6 mM $FeCl_2$ and 900 µL of methyl alcohol (≥99.93%). After incubation for 5 min, 100 µL of 5 mM ferrozine was added, and the mixture stirred and allowed to react for 10 min, allowing the residual iron complexation. The absorbance of the Fe^{2+}/Ferrozine complex was assessed at 562 nm ($A_{562\,nm}$). The percentage of chelating activity was expressed as follows:

$$Chelatingactivity(\%) = [(A_c - A_t)/\mathrm{A_c})] \times 100, \quad (3)$$

where A_c and A_t refer to the absorbance of the standard and the sample, respectively. For this activity, the chelating agent ethylenediaminetetraacetic acid (EDTA) was used as a reference.

2.8.3. Reducing power

The reducing power was ascertained according to the method of Yen and Chen (1995) with slight

modification. Briefly, for each sample, 100 µL was mixed with 100 µL of buffer E and 100 µL of potassium ferricyanide (0.1 g/L). The mixture solution was incubated for 20 min at 50 °C. After incubation, 100 µL of 100 g/L trichloroacetic acid, as precipitation agent, was added. This reaction mixture was centrifuged (15,000 rpm for 10 min at 4 °C), 100 µL of the upper layer mixed with 100 µL of distilled water and 200 µL of 100 mg/L ferric chloride and allowed to stand for 10 min at 25 °C. The absorbance was determined at 700 nm ($A_{700\,nm}$). The results were expressed in mg EAG/100 g DM as determined from using a trolox calibration curve.

2.8.4. Hydroxyl radical scavenging

The hydroxyl radical removal test was performed as previously described, but with a few modifications (Li et al. 2008): 1 mL of 1,10-phenanthroline monohydrate (0.75 mM) as a metal chelator, 2 mL of buffer F, and 1 mL of $FeSO_4$ (0.75 mM) were thoroughly mixed with 1 mL of H_2O_2 (0.12%) and 1 mL of *Lactobacillus fermentum* cells containing 10^6–10^9 colony forming unit (CFU)/mL. The mixture was incubated for 90 min at 37 °C, and the absorbance was determined at 536 nm ($A_{536\,nm}$) as follows:

$$Hydroxylradicalscavengingactivity(\%) = [(A_s – A_c)/(A_b - A_c)] \times 100, \quad (4)$$

where A_s, A_c, and A_b indicates the absorbance of the sample, the control solution (1,10-phenanthroline, $FeSO_4$, and H_2O_2), and the blank solution (1,10-phenanthroline and $FeSO_4$), respectively.

2.9. Statistical analyses

The biochemical and antioxidant results were analysed using Microsoft Excel (version 2007, Microsoft Inc. USA) and Graph Pad PRISM 5 software (version 5.03), respectively. All values correspond to the mean of three independent replicates with their standard deviation (mean ± SD). The analysis of variance (ANOVA) with the lower significant dissimilarity assay was used to ascertain the significant differences ($p < 0.05$) among the means. The correlation coefficient between the studied parameters was calculated with correlation of data using the correlation matrix and the significance degree of the data is considered at probability ($p < 0.05$).

3. Results and discussion

3.1. Peroxidase extraction and purification

Over the years, horseradish tubers have been the only commercial source for peroxidase production. However, peroxidases from microorganisms and plants can also provide peroxidases with similar or even better substrate specificities, stability, yield, and techno-economic feasibility (Walwyn et al. 2015; Mbadinga Mbadinga et al. 2020). Therefore, numerous investigations focussed on peroxidases from different origins are being carried out in order to improve already existing analytical procedures and/or the development of new ones (Fortea et al. 2009). Again, by purifying a peroxidase, it can be clearly established that the particular enzymatic activity actually resides in a unique protein. Thus, the purified protein serves as extremely valuable biochemical reagent. In this study, the TRP was purified to homogeneity from the Algerian white turnip roots using $(NH_4)_2SO_4$ saturation (30%–80%) followed by gel filtration chromatography using a Sephacryl® S-200 HR column and the fractions with peroxidase activity eluted at 1.2 void volume (Figure 1(A)). Final purification was achieved by ion-exchange chromatography (Mono Q-Sepharose®) where the TRP activity was eluted at 150mM–220 mM NaCl (Figure 1(B)).

The purification steps of the enzyme are summarised in Table 1. From the Mono Q-Sepharose® step TRP was eluted from fractions 56–72 (Figure 1(B)), with an RZ value of 2.9 acquired for the final step, indicating a very high level of purity. These purification steps of TRP complement several studies, which have previously demonstrated that saturation with ammonium sulphate has been used for the purification of HRP (Thongsook and Barrett 2005), the peroxidase from cabbage leaves (Zeyadi 2019), and the peroxidase from Turkish black radish (Oztekin et al. 2019). In addition, the NaCl gradient elution of the POD purified from Indian turnip roots gave a single peak (Singh and Singh 2003). The specific activity of TRP (743.77 U/mg), is higher compared to others described in literature. In fact, it is in harmony with that obtained from horseradish roots of *A. rusticana* (772 U/mg) (Lavery et al. 2010). However, it is lower than that of peroxidase from red beet (10,500 U/mg) (Liu et al. 2008). The partially purified peroxidase from the Iranian turnip, *Brassica rapa*, showed a specific activity of 5170.47 U/mg and 1816.82 U/mg when two different purification protocols were used (Motamed et al. 2009). The elevated specific activity established the great potential of the TRP for application in

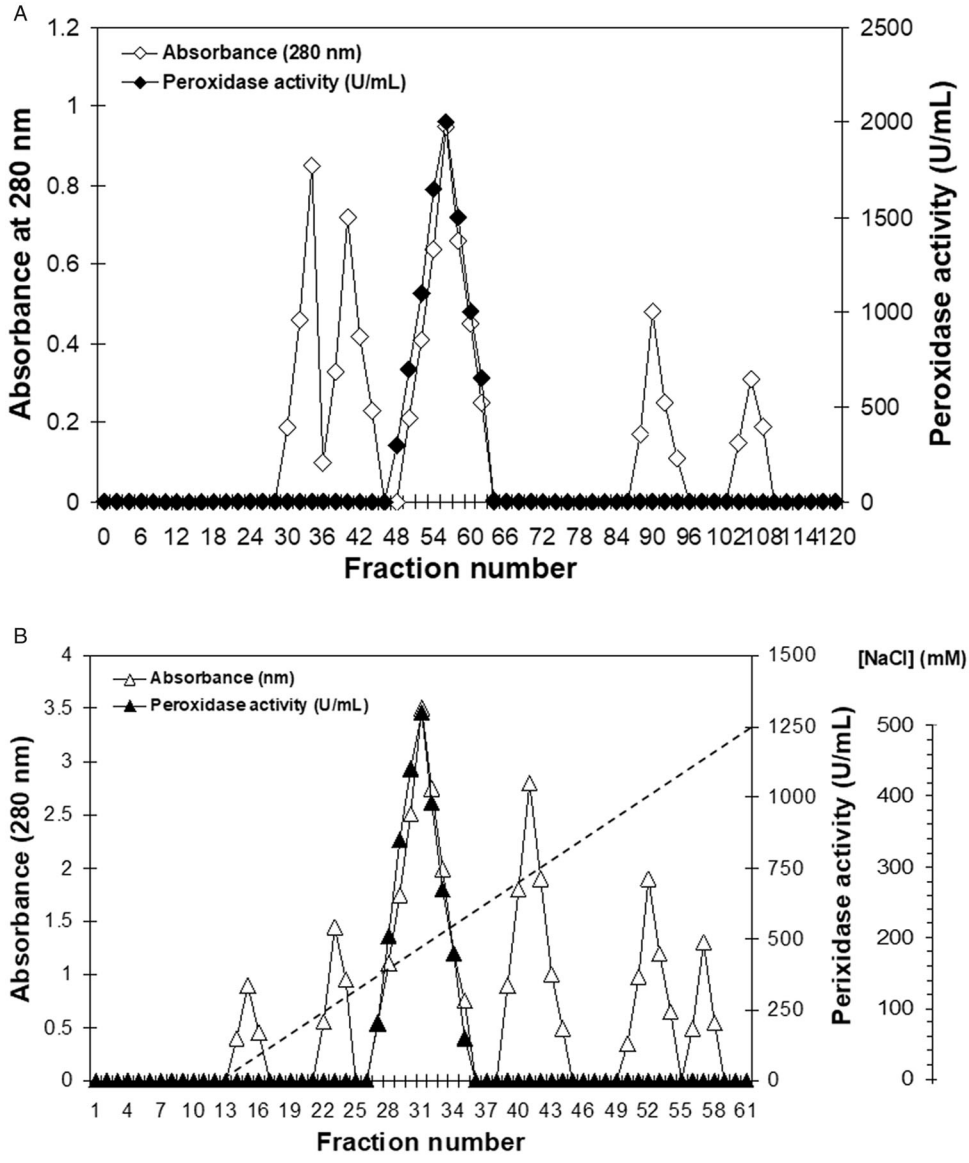

Figure 1. Purification of the TRP enzyme from Algerian white turnip roots, *B. rapa*, variety *rapa*. (A) Elution profile of TRP on Sephacryl® S-200 HR column equilibrated with the buffer B. (B) Chromatography profile of the purified peroxidase on Mono Q-Sepharose® anion exchanger equilibrated with the buffer C. The adsorbed material was eluted with a linear NaCl gradient (from 0 mM to 500 mM) in buffer C at a rate of 0.5 mL/min, and examined for protein concentration and peroxidase activity at 280 nm and 470 nm, respectively.

various industrial and therapeutic processes as well as the potential to substitute the HRP commercial peroxidase.

3.2. Molecular weight determination and zymography of TRP

TRP was purified to a homogeneous state and analysed with SDS-PAGE. Its molecular weight was determined to be about 58 kDa (Figure 2(A)). The zymography staining activity of the TRP, with guaiacol, demonstrated a unique band in proportion to the position of the peroxidase activity (Figure 2(B)). Further, a high purity in the enzyme preparation was shown as it exhibited an individual elution peak at retention time (R_t) of 10.20 min, which is equivalent to a single protein of ~58 kDa (Figure 2(C)). The molecular weight of TRP is comparable with other PODs having molecular weights in the range of 35 kDa–95 kDa. In fact, Kalin et al. (2014), found that the POD purified from Turkish turnip roots had a molecular weight of 65.8 kDa (Somtürk et al. 2014). Other PODs molecular weights from other plant species has been reported as follow: rosemary, 33 kDa (Aghelan and Shariat 2015), garlic, 36.5 kDa (Marzouki et al. 2005), chickpea, 39 kDa (Bhatti et al. 2006), horseradish root, 40 kDa (Lavery et al. 2010), avocado, 40 kDa (Rojas-Reyes et al. 2014), chickweed flower, 44 kDa (Yan et al. 2015), wind

Table 1. Purification steps followed for the isolation and purification of TRP from Algerian white turnip roots.

Purification step	Total activity (units)[a]	Total protein (mg)[a,b,c]	Specific activity (U/mg)[a]	Activity yield (%)	Purification factor (*n*-fold)	RZ
Crude extract	950,000 ± 3,895	1,250 ± 18	760	100	1	NP
$(NH_4)_2SO_4$ (30%–80%)	826,500 ± 3,250	670 ± 9	1234	87	1.6	NP
Gel-filtration chromatography (Sephacryl® S-200 HR)	693,500 ± 2,735	215 ± 4	524.5	73	2.8	1.1
Ion-exchange chromatography (Mono Q-Sepharose®)	485,750 ± 1,800	33.5 ± 1	14,500	51.1	19	2.9

[a]The assays were performed in triplicate and the ± standard errors (SE) are indicated.
[b]Unit definition is provided in Section 2.3.
[c]Protein concentration was assessed with a Bio-Rad Dc protein assay kit.
NP: No peak at $A_{400\,nm}$.

palms, 50 kDa (Caramyshev et al. 2006), artichoke, 57 kDa (Cardinali et al. 2011), red cabbage, 69.3 kDa (Zeyadi 2019), and black cabbage, 95 kDa (Somtürk et al. 2014).

3.3. N-terminal sequence of the TRP

The 19 first amino acid residues of the N-terminal sequence were ascertained to be QLTPTFLNNSCPNVSNIVR (Table 2) and displayed a high identity with HRP C1 extracted from *A. rusticana* (88.47% of identity). This data clearly suggested that the TRP enzyme from *B. rapa*, variety *rapa*, is a novel POD.

3.4. Biochemical and spectral characterisation of TRP

3.4.1. Spectral characterisation of a haem cofactor

Throughout the purification process, a russet colour was detected for the soluble active fractions, demonstrating that a chromogenic cofactor was linked with the peroxidase. The spectral properties of the purified enzyme showed that TRP has an aromatic amino acid peak at 280 nm and a haem-compound peak at 406 nm. The ratio of the absorbance values represents the RZ of the TRP enzyme to be 2.9, which was similar to other PODs (Regalado et al. 1996; Hamed et al. 1998; Duarte-Vazquez et al. 2001; Dalal and Gupta 2010; Kalin et al. 2014). These results clearly indicate that TRP contains a haem cofactor that utilises H_2O_2 as the electron acceptor to catalyse various oxidative reactions.

3.4.3. Effect of guaiacol, H_2O_2, and 4-aminoantipyrine on the TRP activity

The data presented in Figure 3 shows that the optimum activity for TRP is observed at a concentration of 45 mM guaiacol (Figure 3(A)), 0.5 mM H_2O_2 (Figure 3(B)) and 25 mM 4-aminoantipyrine (Figure 3(C)) with an optimal TRP concentration of 10 µg/mL, which is in accordance with reports on other PODs (Bouazizi et al. 2008; Simonetti et al. 2009; Dalal and Gupta 2010; Kalin et al. 2014; Basha and Prasada Rao 2017; Gracas et al. 2020). Oxidation of guaiacol leads to tetraguaiacol formation. This reaction exhibits classical Michaelis-Menten kinetics. In fact, the peroxidase activity was increased with increasing concentrations of guaiacol. It should be noted, however, that at 45 mM of guaiacol, an apparent saturation of activity was observed (Figure 3(A)). This behaviour was similar to 4-aminoantipyrine at 25 mM (Figure 3(C)).

H_2O_2 was further noted to inhibit TRP activity, which were comparable to reports on other PODs (Prat et al. 1991). For the purified TRP, the change in the absorbance at 470 nm was not observed in the absence of H_2O_2 indicating that the activity of phenol oxidase (PhO) is negligible. Figure 3(D) illustrates the dependence of enzyme activity in the assay mixture over a range of incubation time for three concentrations of TRP peroxidase. In all cases, the peroxidase activity, ascertained by assessing the tetraguaiacol formation at 470 nm, is significant at 10 µg/mL. Furthermore, the rate of tetraguaiacol formation was linear relative to the time reaction.

3.4.4. Effect of selected inhibitors and metal ions

TRP are completely inhibited by 1 mM, 10 mM or 15 mM of KCN and NaN_3, well-known inhibitors of peroxidases (Table 3). This result suggests that a haem component is involved in the catalytic activity of the TRP enzyme. The β-ME or DL-DTT and SDS contribute to the reduction of disulphide bonds and destroyed the protein hydrophobic effect to affect the protein tertiary, or quaternary structure, causing the degeneration. Moreover, the addition of 1 mM DL-DTT, 5 mM β-ME, and 30 mM SDS had less inhibitory effect on TRP activity retaining 35%, 30%, and 26% of its initial activity, respectively. Therefore, the TRP enzyme had a strong tolerance to DL-DTT, β-ME, and SDS.

A variety of metal ions (2 mM) were also evaluated in terms of their effect on the activity of the TRP enzyme (Table 4). Additionally, our data show that the

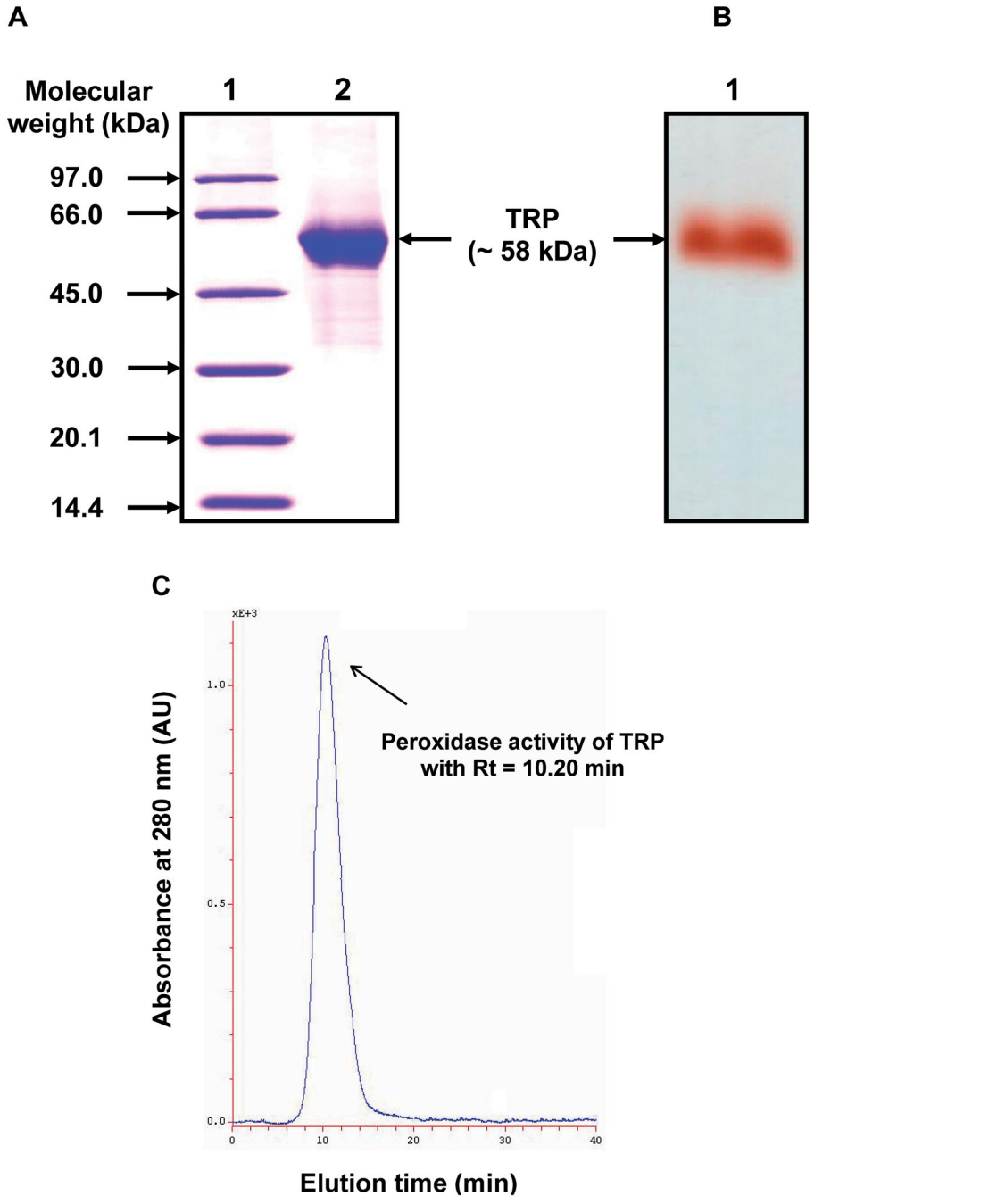

Figure 2. Electrophoresis and HPLC profiles of TRP from Algerian white turnip roots, *B. rapa*, variety *rapa*. (A) 12% SDS-PAGE of TRP enzyme. Lane 1, the Amersham LMW protein marker; Lane 2, the purified TRP obtained after Mono Q-Sepharose® chromatography (fractions 150 mM-200 mM NaCl) (50 µg). (B) Zymography with guaiacol staining of TRP activity. Lane 1, the purified TRP obtained after Mono Q-Sepharose® chromatography (fractions 150 mM-220 mM NaCl) (50 µg). (C) Chromatography profile of the purified TRP enzyme with Protein® WK-802.5 HPLC column, equilibrated with buffer B and native protein markers of 670 kDa, 158 kDa, 44 kDa, 17 kDa, and 13.5 kDa, shows a single peak of ∼58 kDa. The proteins were divided by isocratic elution at a rate of 0.5 mL/min with buffer B and measured at 280 nm. The pure TRP enzyme, with R_t of 10.20 min, exhibited peroxidase activity.

TRP activity was entirely inhibited by the nickel, cadmium, and mercury ions since it correlates with thiol (–SH) groups of the cysteine residues and disturb its 3 D configuration as reported for others PODs (Bouazizi et al. 2008; Simonetti et al. 2009; Dalal and Gupta 2010; Kalin et al. 2014; Basha and Prasada Rao 2017; Gracas et al. 2020) and fungal peroxidases (Bouacem et al. 2018; Rekik et al. 2019; Bouacem et al. 2021). Furthermore, TRP activity was significantly enhanced by the addition of 2 mM of manganese

Table 2. Alignment of the N-terminal sequence amino acid residues of TRP from Algerian turnip roots with that of the sequences of other PODs.

Peroxidase	Plant origin	N-terminal amino-acid sequence[b]	Identity (%)
TRP (this study)	*Brassica rapa*, variety *rapa*	QLTPTFLNNSCPNVSNIVR[a]	–
HRP isoenzyme_25148.1(C1C) (Genbank accession no.: CCJ34821)	*Armoracia rusticana*	QLTPTF**YD**NSCPNVSNIVR	88.47
PRX33 (Genbank accession no.: XP_006291394)	*Capsella rubella*	QLTPTF**YD**NSCPNV**T**NIVR	84.21
PRX34-like (Genbank accession no.: XP_013656048)	*Brassica napus*	QLTPTF**YDS**SCPNV**T**NIVR	78.95
PRX32 (Genbank accession no.: XP_002877238)	*Arabidopsis lyrata* subsp. *lyrata*	QLTPTF**YD**N**T**CPNV**FT**IVR	73.68
PRX E5 (Genbank accession no.: XP_002299152)	*Populus trichocarpa*	QLTPTF**YDET**CPNVS**S**I**I**R	68.42

[a]This sequence was submitted to BLASTP in order to identify the top hits to the query sequence.
[b]Residues not matching with the TRP enzyme are highlighted in bold.

(180%), magnesium (151%), and calcium (137%) ions.

The Mn^{2+} treatment increased peroxidase activity, suggested that this cation contribute to regulating the enzyme active conformation and thus enhanced the TRP activity.

3.4.5. Evaluation of the effect of different pH on peroxidase activity and stability

The purified TRP is active over a pH range of 2–11 with most activity observed in the acidic region at pH 6 (Figure 4(A)). The relative TRP activities at pH 4 and

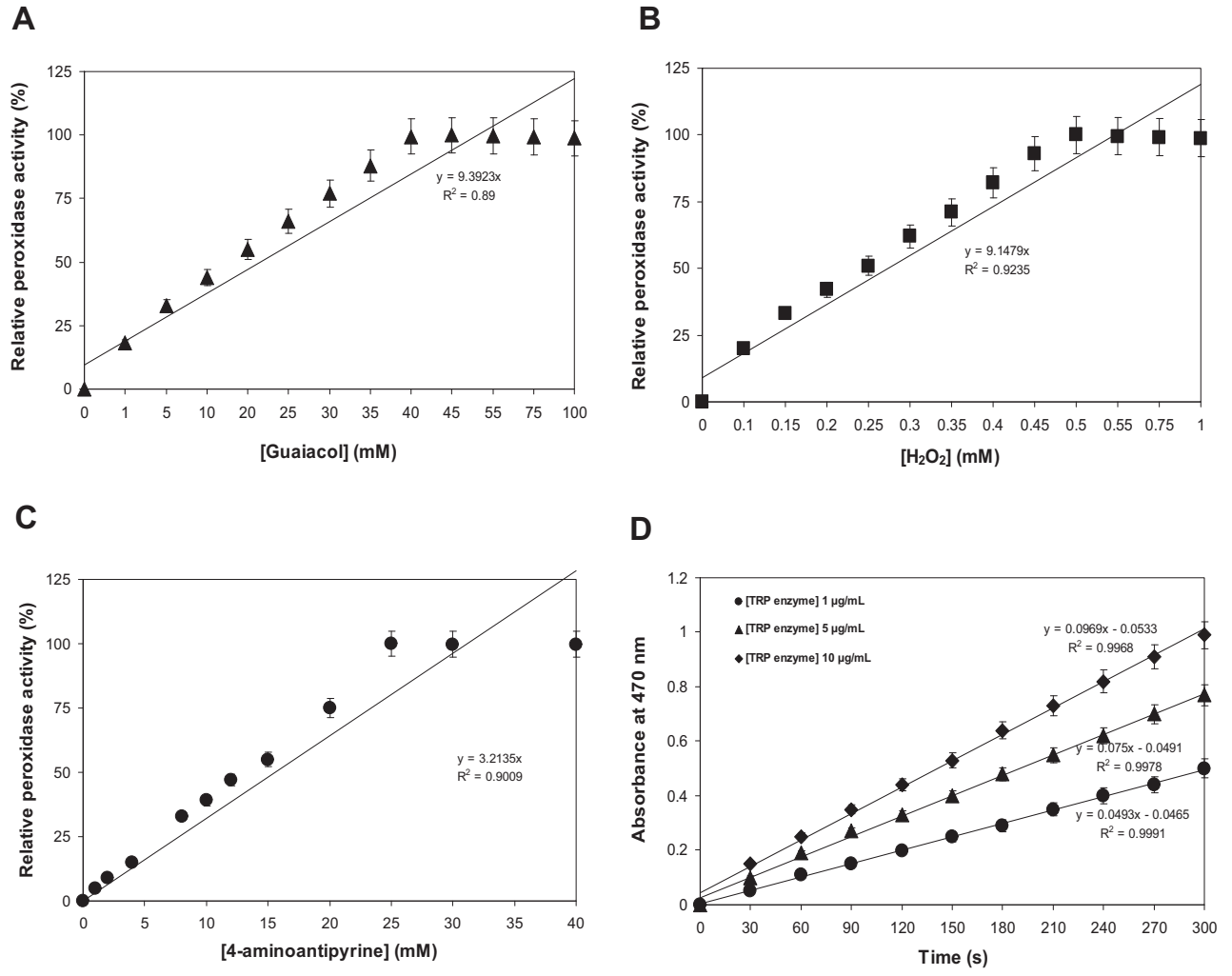

Figure 3. Enzyme reaction operating condition rates. (A) Effect of guaiacol on TRP activity. The TRP activity was assessed with a guaiacol concentration range from 0 mM to 100 mM. (B) Effect of H_2O_2 on TRP activity. The TRP activity was assessed with H_2O_2 concentrations ranging from 0.1 mM to 1 mM. (C) Effect of 4-aminoantipyrine on TRP activity. The TRP activity was assessed with a 4-aminoantipyrine concentration range of 1 mM–40 mM. (D) Effect of reaction time on TRP activity. The absorbance at 470 nm was assessed with different TRP concentrations: 1 µg/mL, 5 µg/mL, and 10 µg/mL at a reaction time of 0 min to 300 min. Each point symbolises the mean ($n = 3$) ± SD.

Table 3. Effect of a variety of inhibitors and specific reagents (tested at different concentrations) on the TRP from Algerian white turnip roots using guaiacol as a substrate.

Inhibitor/reagent	Concentration (mM)	Residual peroxidase activity of TRP (%)[a,b]
Control	–	100 ± 2.5
KCN	5	0 ± 0.0
	10	0 ± 0.0
	15	0 ± 0.0
NaN3	5	0 ± 0.0
	10	0 ± 0.0
	15	0 ± 0.0
L-cystine	1	12 ± 0.3
	2	11 ± 0.3
	5	10 ± 0.3
Hydroxylamine	1	8 ± 0.2
	2	7 ± 0.2
	5	5 ± 0.2
DTNB	5	98 ± 2.5
	10	95 ± 2.4
	15	91 ± 2.3
NEM	1	104 ± 2.6
	2	101 ± 2.5
	5	99 ± 2.5
Iodoacetamide	2	101 = 2.5
	5	96 = 2.4
	10	93 = 2.3
SDS	20	77 ± 2.2
	30	74 ± 2.2
	40	70 ± 1.1
β-ME	2	75 ± 2.2
	5	70 ± 2.1
	10	66 ± 1.9
DL-DTT	0.5	69 ± 2.1
	1	65 ± 1.9
	2	60 ± 1.7

[a]The assays were performed in triplicate and the ± SE is indicated.
[b]The TRP activity calculated in the absence of inhibitor was considered as the control and taken as 100%.

Table 4. Effect of selected metal ions on the activity of the TRP from Algerian white turnip roots. Guaiacol was used as the substrate.

Metal ion at 2 mM	Origin	Residual peroxidase activity of TRP (%)[a,b]
Control	–	100 ± 2.5
Mn^{2+}	$MnSO_4$	180 ± 3.8
Mg^{2+}	$MgSO_4$	151 ± 3.6
Ca^{2+}	$CaCl_2$	137 ± 3.1
Cu^{2+}	$CuSO_4$	105 ± 2.6
Ba^{2+}	$BaCl_2$	90 ± 2.2
Fe^{2+}	$FeSO_4$	77 ± 2.2
Zn^{2+}	$ZnCl_2$	40 ± 1.4
Co^{2+}	$CoCl_2$	25 ± 1.0
Ni^{2+}	$NiCl_2$	0 ± 0.0
Cd^{2+}	$CdCl_2$	0 ± 0.0
Hg^{2+}	$HgCl_2$	0 ± 0.0

[a]The assays were performed in triplicate and the ± SE is indicated.
[b]The TRP activity calculated in the absence of metal ions was considered as control (designated as 100%).

9 were determined as 75% and 55%, respectively. Turnip peroxidase has an advantage: in comparison to the commercial HRP enzyme, TRP can be utilised in an acidic environment, in which HRP cannot operate properly. For comparison, PODs from *B. rapa* and *A. rusticana* roots exhibited maximum activity at pH 4 and 7, respectively. The POD from *Copaifera angsdorffii* leaves showed optimal activity at pH 6 (Maciel et al. 2007). Furthermore, our previous study on the POD crude extract from the turnip of the same variety revealed an optimal activity at pH 6 (Dahdouh et al. 2020).

The TRP is stable at pH 4–8 (Figure 4(B)). The half-life of TRP at pH 4, 5, 6, 7, and 8 was 12 h, 9 h, 7 h, 5 h, and 3 h, respectively. The pH stability profile of TRP allows for different industrial applications that require acidic conditions. The effect of different pH on activity and stability of TRP demonstrate that this enzyme is more efficient to the peroxidase already described (Motamed et al. 2009). In fact, the optimum activity of TRP is observed at pH 6 with relative activity at pH 9 of 55% compared to pH 4 for the reported partially purified turnip peroxidase previously described with relative activity at pH 9 of 45% (Motamed et al. 2009).

3.4.6. Assessment of the effect of different temperatures on peroxidase activity and stability

At pH 6, the optimum temperature for the TRP is 45 °C (without Mn^{2+}) and 55 °C with Mn^{2+} at 2 mM (Figure 4(C)). The optimum temperature of TRP is lower than that of the POD from *C. angsdorffii* leaves that exhibit maximum activity at 35 °C (Motamed et al. 2009).

We then proceeded to determine whether these effects occurred through alterations in the half-life of the TRP peroxidase. The half-life of the TRP at 40 °C, 50 °C, and 60 °C without Mn^{2+} are 10 h, 6 h, and 3 h, respectively (Figure 4(D)). Nevertheless, with 2 mM Mn^{2+}, the half-life of TRP led to an increase respectively to 12 h, 8 h, and 5 h. The thermo-stability of TRP was superior to other PODs from *B. rapa* and *A. rusticana* roots (Lueangjaroenkit et al. 2020; Pech-Canul et al. 2020; Rajhans et al. 2020; Yang et al. 2020). The effects of temperature on the activity and stability of TRP demonstrate that this enzyme is more efficient to the previously described partially purified turnip peroxidase (Motamed et al. 2009). In fact, the optimum activity of TRP is attained at 55 °C compared to 35 °C for the related peroxidase reported elsewhere (Motamed et al. 2009).

These properties support the fact that TRP has potential for application in the food industry.

3.5. Determination of kinetic parameters

The kinetic parameters are summarised in Table 5. The enzymes (TRP and HRP) displayed conventional Michaelis-Menten kinetics for the four substrates guaiacol, pyrogallol, catechol, and anisole (data not

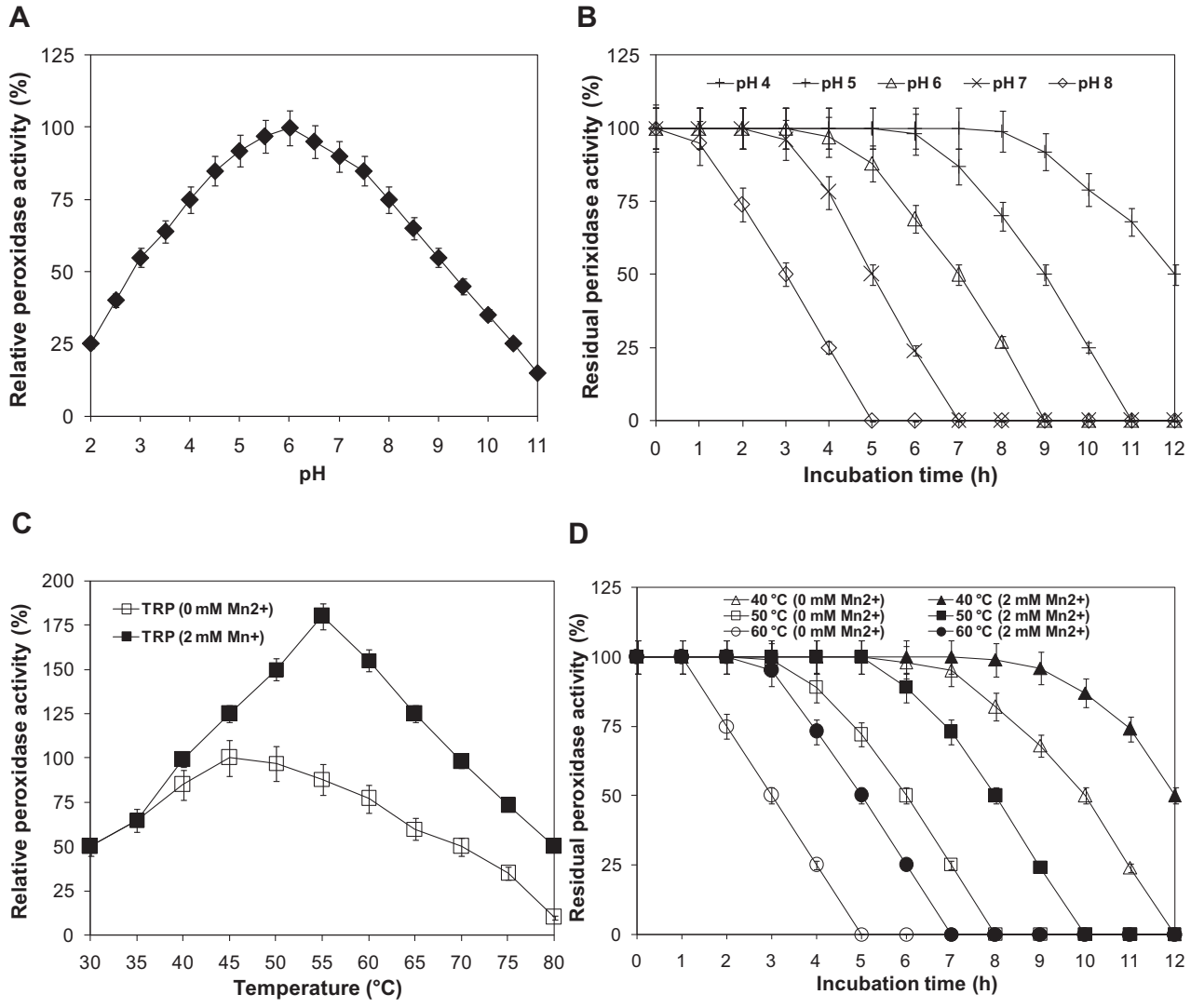

Figure 4. Evaluation of the effects of pH and temperature on the activity and stability of the purified TRP enzyme from Algerian turnip roots, *B. rapa*, variety *rapa*. (A) The TRP pH activity was assessed across a pH range of 2–11 using buffers of different pH levels and guaiacol as the substrate. (B) The TRP pH stability was ascertained by incubating TRP for 12 h in various buffers at 40 °C, and the remaining TRP activity calculated under the standard assay conditions. The activity of TRP prior to incubation was taken as 100% and used as a control. (C) The effect of temperature on the activity of TRP was assessed for 5 min at 30 °C–80 °C at pH 6 and with and without 2 mM Mn^{2+}. (D) The thermo-stability of TRP was examined by incubating TRP for 12 h at different temperature values (40 °C, 50 °C, and 60 °C) with and without 2 mM Mn^{2+}. The activity of the untreated TRP was considered as 100%. Vertical bars designate ± SE of the mean ($n = 3$). All results are expressed as mean of at least three independent assays.

shown). The k_{cat}/K_m values for the four substrates for each POD was similar, i.e. guaiacol > pyrogallol > catechol > anisole. The k_{cat}/K_m values of TRP were 4.28, 3.99, 2.86, and 1.97-fold higher than that of HRP for guaiacol, pyrogallol, catechol, and anisole, respectively. The data clearly suggest that TRP is ideal for application in the food industry and various other biotechnological applications.

3.6. Antioxidant activities

The purification steps resulted in the enhancement of the specific activity of the purified TRP, which is mainly due to the removal of contaminating total proteins/enzymes. The antioxidant properties of the TRP fractions prepared at different stages of purification were evaluated accordingly for their capacity for radical scavenging (ABTS and OH), their chelating effect on Fe^{2+} and their reducing power. For each activity, BHT was used as a standard control, excluding the chelating capacity of the ferrous ion where EDTA was used.

3.6.1. ABTS radical scavenging activity

ABTS radical recovery activity is used to estimate the total antioxidant activity of antioxidants (Payet et al. 2005). From the results presented in Figure 5(A),

Table 5. Kinetic parameters of TRP and HRP towards guaiacol, pyrogallol, catechol, and anisole as substrates.

Substrate	Enzyme	K_m (mM)	V_{max} (U/mg)	k_{cat} (min^{-1})	k_{cat}/K_m (min^{-1} mM^{-1})
Guaiacol	TRP	0.139 ± 0.01	14,500 ± 210	9,667 ± 140	69,547
	HRP	0.302 ± 0.02	7,350 ± 107	4,900 ± 71	16,225
Pyrogallol	TRP	0.195 ± 0.01	13,485 ± 194	8,990 ± 129	46,103
	HRP	0.388 ± 0.03	6,710 ± 97	4,473 ± 65	11,528
Catechol	TRP	0.250 ± 0.02	12,325 ± 177	8,217 ± 120	23,868
	HRP	0.447 ± 0.03	5,590 ± 81	3,727 ± 54	8,338
Anisole	TRP	0.406 ± 0.04	8,159 ± 118	5,439 ± 78	13,396
	HRP	0.491 ± 0.05	4,991 ± 71	3,327 ± 48	6776

Values represent the means of a three independent replicates, and the ± SE is indicated.

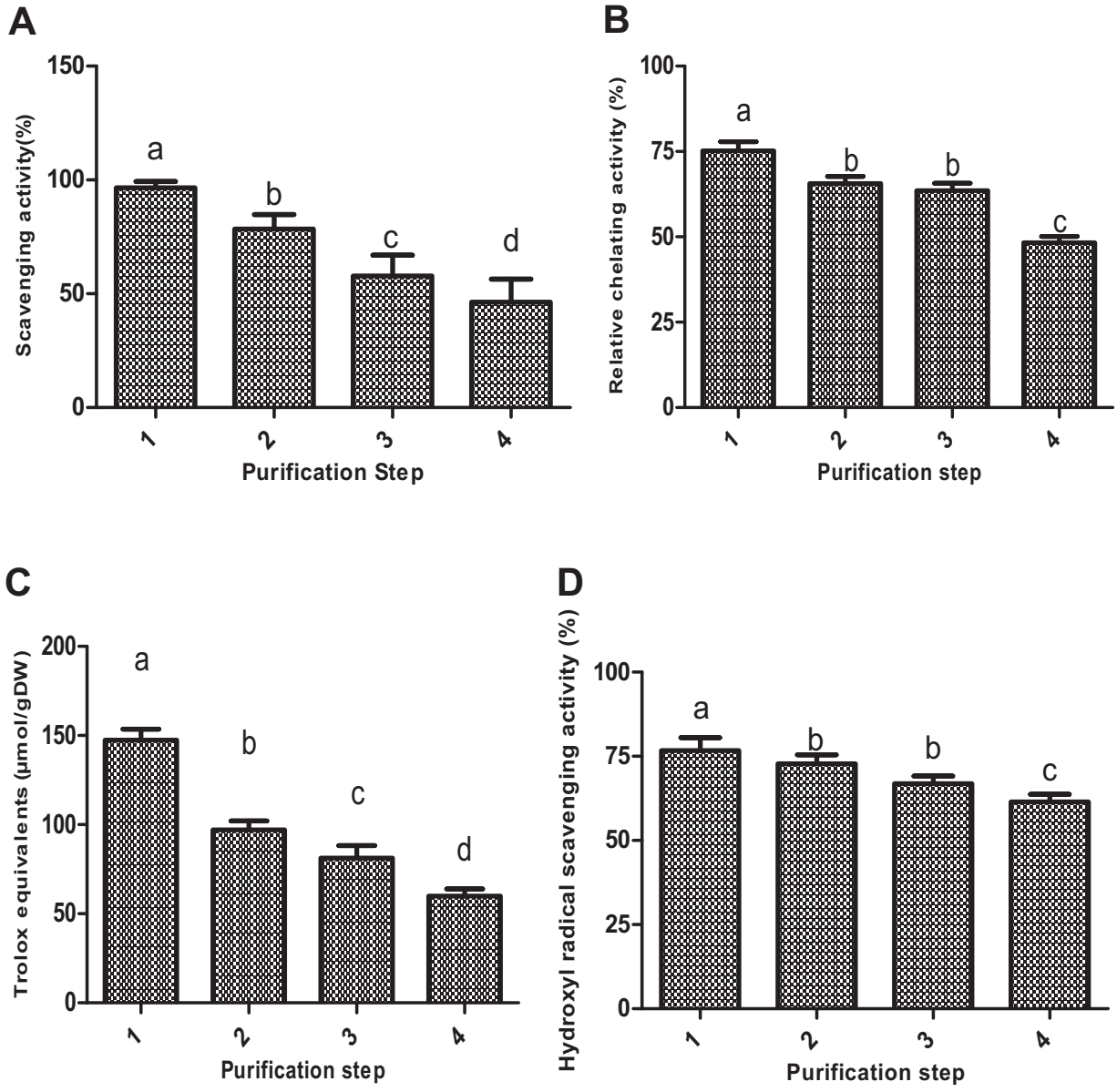

Figure 5. Antioxidant potential of the TRP from the Algerian white turnip (*B. rapa*, variety *rapa*) roots. (A) Antioxidant capacity of ABTS radical scavenging power, (B) Metal chelating effect, (C) Reducing power, and (D) Hydroxyl radical ($^{\bullet}OH$) scavenging (1, 2, 3, and 4 correspond to the purification steps outlined in Table 1). Each value represents the mean ± SD ($n = 3$). The small letters a, b, c, and d, designates considerable differences for the given sample between the dissimilar purification stages ($p < 0.05$); with a > b > c > d.

depending on the purification steps, the ABTS anti-free radical activity of the enzyme fractions diminishes significantly ($p < 0.05$) depending on the purification steps. Moreover, we detected an 50% decrease of ABTS anti-free radical activity compared to that of the crude homogenate. The values of the antioxidant

activities oscillate between 96.54% and 46.32%. This difference may therefore be the result of a synergistic effect of the bioactive peptides and polyphenols present in the crude extract. It is well documented that *B. rapa*, variety *rapa* is an appreciable source of phenolic compounds, in particular flavonoids (Cartea et al. 2010). The antioxidant capacity of enzymatic fractions could be allocated to the presence of some amino-acid residues (Met, His, Trp, Phe, Tyr, Leu, Pro, and Gly) (Mechri et al. 2020a). On the other hand, the removal of certain proteins and peptides of LMW has the effect of reducing the antioxidant activity.

3.6.2. TRP chelating power

Iron bound to proteins, e.g. transferring, or detained in storage as ferritin in a redox state can cause overloading of iron in the human body and require the consumption of exogenous chelators to avoid the build-up of free iron. These exogenous chelators can be found in the form of a variety of antioxidants in food (Sellem et al. 2016; Mechri et al. 2020a). The results of the chelating analyses, as shown in Figure 5(B), shows that the fractions of steps (E2, E3, and E4) were significantly decreased ($p < 0.05$) compared with the first step (E1). More specifically, the activity of the crude extract being the highest (75.23%), and the lowest activity was observed in the pure enzymatic fraction (48.32%). This activity might be connected to the Gly- and His-rich peptides (Xu and Chance 2007; Liu et al. 2016) and reflects the complex nature of the extract, which may include various iron chelators, with dissimilar iron affinities. The decrease in the chelating activity of protein fractions is therefore relative to the presence of these amino acids (Papuc et al. 2017).

3.6.3. Reducing power

The reducing power was determined by measuring the reduction of the Fe^{3+}/Ferricyanide complex in ferrous form, specified the implications of the most frequently observed chemical mechanisms, namely the donation of electrons/hydrogen (Mechri et al. 2020b). In this study, the reducing power in all fractions ensuing from (precipitation and inhibition with PVPP), ultrafiltration, and anion exchange chromatography was significantly ($p < 0.05$) lower compared with the crude homogenate (Figure 5(C)). The reduction power values of the fractions from the different purification stages vary between 130.76% and 52.96% trolox equivalents (μmol/g DM). High levels of reducing power indicate the presence of certain compounds capable of donating electrons to free radicals, thereby reducing oxidative stress.

3.6.4. Hydroxyl radical scavenging

The hydroxyl radical is the main reactive free radical, and it can be produced from a superoxide anion and H_2O_2 in the presence of metal ions (Csire et al. 2020). The hydroxyl radical can react with macromolecules, such as proteins, amino-acids, lipids, and DNA (Umeno et al. 2017). The free ROS have a significant function in the metabolism and development of aerobic organisms, but their uncontrolled production leads to oxidative stress. Indeed, an excess of free radical production in living cells has been revealed to be accountable for substitutions and carcinogenesis by inducing base alteration and DNA strand breakage. The activity trapping of the hydroxyl radicals by the enzyme fractions decrease significantly ($p < 0.05$) depending on the purification steps (Figure 5(D)). The hydroxyl radical ($^{\bullet}OH$) scavenging activity does not present much difference between purification steps; the values oscillated between 76.71% and 61.49%. Accordingly, TRP can be applied in the form of enzyme therapy in the pharmaceutical, cosmetic, and medicinal industries, with biological eradication of free radicals, e.g. ABTS and OH. Similar studies on soy protein hydrolysates reported that they had the highest hydroxyl trapping capacity (69.75%) (Zhuang et al. 2013). In addition, the use of natural protein extracts or purified proteins as antioxidants has been identified. Proteins isolated from soybeans, mushrooms, corn zein, potato, yam, chickpeas, and white beans are said to have antioxidant activity (Li 2008). The proteins' antioxidant activity depends on the nature and composition of their amino acid residues. It has been described that an elevated percentage of hydrophobic amino acids in proteins can enhance their lipid solubility and thus assist access to free radicals present in the lipid phase (Qian et al. 2008). For example, the antioxidant activities of tyrosine and phenylalanine are due to their ability to donate protons to free radicals, and tryptophan includes the indole group that acts as an aromatic heterocyclic organic compound, and it can donate hydrogen in order to reduce the radical response (Qian et al. 2008). In contrast, the basic (lysine and arginine), and acidic (aspartate, and glutamate) amino acid residues exert antioxidant activity by chelating metal ions. In addition, proline residues of peptides are significant for the elimination of radicals because of its structure, while histidine can donate protons to electron-deficient radicals and improve the trapping capacities of radicals. It also acts as a metal chelator due to its imidazole (Xu and Chance 2007; Liu et al. 2016). It is therefore clear that various factors could influence the antioxidant ability of PODs, including

amino acid content, substrate affinity, polarities, and structures (Jahangoshaei et al. 2015).

4. Conclusions

Due to their potential application, the POD group of enzymes have become a main focus area in the field of traditional medicine and pharmaceutical industry. To use these enzymes in such domains, it is very important to maintain activity and for the enzymes to exhibit a temperature stability over a wide pH range as well as a noteworthy antioxidant activity. In the current study we have established an easy procedure for the purification of TRP from the roots of the Algerian white turnip, *B. rapa*, variety *rapa*, to homogeneity followed by the determination of its promising biochemical properties and high antioxidant potential which has not been reported before. The characteristics of this biocatalyst indicate that TRP could be an essential tool for a variety of applications mainly in the pharmaceutical industry as a key antioxidant biocatalyst. Further investigations, focussed on understanding the signalling properties and structure-function of TRP, are still required in order to assess how the enzyme is responsible for the observed potential activities that can negate oxidative stress. Additional studies will be required in order to evaluate the cytotoxicity effect and in vivo activities of TRP. Molecular docking and site-directed mutagenesis approaches will also be required in order to investigate the structure-function relationships of this enzyme and other PODs.

Disclosure statement

No potential conflict of interest was reported by the author(s).

Acknowledgments

The authors want to express their sincere gratitude to Dr. M. Le Roes-Hill from the Applied Microbial and Health Biotechnology Institute, Cape Peninsula University of Technology (Bellville, South Africa) and Mr. H. Gwaithan from the Department of Bioprocess Technology, Faculty of Biotechnology and Biomolecular Sciences at the Universiti Putra Malaysia (UPM), Serdang, Kuala Lumpur, Malaysia for English editing and proofreading services.

Funding

This study was financially supported by the Direction Générale de la Recherche Scientifique et du Développement Technologique (DGRSDT) and the Direction Générale des Enseignements et de la Formation Supérieure (DGEFS) in the Ministry of Higher Education and Scientific Research (MHESR) in Algeria under the National Research Project P RFU no.: D00L01UN060120190003, the Multilateral Project Partenariats Hubert Curien (P HC)-Maghreb 2020 Program (FranMaghZYM 2020-2023, code Campus France: 43791T M & code P HC: 01MAG20), and the Algerian-Tunisian R&I Cooperation for the Mixed Laboratories of Scientific Excellence 2021-2024 (Hydro-BIOT ECH, code LABEX/TN/DZ/21/01).

ORCID

Khelifa Bouacem http://orcid.org/0000-0003-3383-4020
Bassem Jaouadi http://orcid.org/0000-0002-5182-7353

References

Aghelan Z, Shariat SZS. 2015. Partial purification and biochemical characterization of peroxidase from rosemary (*Rosmarinus officinalis* L.) leaves. Adv Biomed Res. 4:159.

Al Ghouleh I, Khoo NKH, Knaus UG, Griendling KK, Touyz RM, Thannickal VJ, Barchowsky A, Nauseef WM, Kelley EE, Bauer PM, Darley-Usmar V, et al. 2011. Oxidases and peroxidases in cardiovascular and lung disease: new concepts in reactive oxygen species signaling. Free Radic Biol Med. 51(7):1271–1288.

Allala F, Bouacem K, Boucherba N, Azzouz Z, Mechri S, Sahnoun M, Benallaoua S, Hacene H, Jaouadi B, Bouanane-Darenfed A. 2019. Purification, biochemical, and molecular characterization of a novel extracellular thermostable and alkaline α-amylase from *Tepidimonas fonticaldi* strain HB23. Int J Biol Macromol. 132:558–574.

Ambatkar M, Mukundan U. 2014. Calcium salts enhance activity and azo dye decolourisation capacity of crude peroxidase from *Armoracia rusticana*. Am J Plant Sci. 5(2):52028.

Basha SA, Prasada Rao UJ. 2017. Purification and characterization of peroxidase from sprouted green gram (*Vigna radiata*) roots and removal of phenol and *p*-chlorophenol by immobilized peroxidase. J Sci Food Agric. 97(10):3249–3260.

Bhatti H, Najma A, Asgher M, Hanif M, Zia M. 2006. Purification and thermal characterization of a novel peroxidase from a local chick pea cultivar. Protein Pept Lett. 13(8):799–804.

Bouacem K, Allala F, Zaraî Jaouadi N, Hamdi S, Mechri S, Ighilahriz K, Rekik H, Hacene H, Bouanane-Darenfed A, Jaouadi B. 2021. A novel peroxidase from white-rot Agaricomycetes fungus *Phlebia radiata* strain KB-DZ15: its purification, characterization, and potential application for dye-decolorization and lignin-biodegradation. Biocatal Biotransform. https://doi.org/10.0.4.56/10242422.2021.1939315.

Bouacem K, Rekik H, Zaraî Jaouadi N, Zenati B, Kourdali S, El Hattab M, Badis A, Annane R, Bejar S, Hacene H, et al. 2018. Purification and characterization of two novel peroxidases from the dye-decolorizing fungus *Bjerkandera adusta* strain CX-9. Int J Biol Macromol. 106:636–646.

Bouazizi H, Jouili H, Geitmann A, El Ferjani E. 2008. Effect of copper excess on H_2O_2 accumulation and peroxidase activities in bean roots. Acta Biol Hung. 59(2):233–245.

Bradford MM. 1976. A rapid and sensitive method for the quantitation of microgram quantities of protein utilizing the principle of protein-dye binding. Anal Biochem. 72: 248–254.

Caramyshev AV, Firsova YN, Slastya EA, Tagaev AA, Potapenko NV, Lobakova ES, Pletjushkina OY, Sakharov IY. 2006. Purification and characterization of windmill palm tree (*Trachycarpus fortunei*) peroxidase. J Agric Food Chem. 54(26):9888–9894.

Cardinali A, Tursi N, Ligorio A, Giuffrida MG, Napolitano L, Caliandro R, Sergio L, Di Venere D, Lattanzio V, Sonnante G. 2011. Purification, biochemical characterization and cloning of a new cationic peroxidase isoenzyme from artichoke. Plant Physiol Biochem. 49(4):395–403.

Cartea ME, Francisco M, Soengas P, Velasco P. 2010. Phenolic compounds in *Brassica* vegetables. Molecules. 16(1): 251–280.

Csire G, Canabady Rochelle L, Averlant Petit MC, Selmeczi K, Stefan L. 2020. Both metal-chelating and free radical-scavenging synthetic pentapeptides as efficient inhibitors of reactive oxygen species generation. Metallomics. 12(8): 1220–1229.

Dahdouh A, Bachir-Bey M, Kati DE. 2020. Optimization of peroxidase activity of turnip (*Brassica rapa*) using response surface methodology. Acta Universitatis Cibiniensis. 24(2): 186–194.

Dahdouh A, Kati DE, Bachir-Bey M, Aksas A, Rezgui F. 2021. Deployment of response surface methodology to optimize microencapsulation of peroxidases from turnip roots (*Brassica rapa* L.) by double emulsion in PLA polymer. J Food Sci. 86(5):1893–1906.

Dalal S, Gupta MN. 2010. Purification and characterization of a peroxidase isozyme from Indian turnip roots. J Agric Food Chem. 58(9):5545–5552.

Dirlewanger E, Cosson P, Tavaud M, Aranzana M, Poizat C, Zanetto A, Arus P, Laigret F. 2002. Development of microsatellite markers in peach [*Prunus persica* (L.) Batsch] and their use in genetic diversity analysis in peach and sweet cherry (*Prunus avium* L.). Theor Appl Genet. 105(1): 127–138.).

Duarte-Vazquez MA, Garcia-Almendarez BE, Regalado C, Whitaker JR. 2001. Purification and properties of a neutral peroxidase isozyme from turnip (*Brassica napus* L. var. purple top white globe) roots. J Agric Food Chem. 49(9): 4450–4456.

Falade AO, Nwodo UU, Iweriebor BC, Green E, Mabinya LV, Okoh AI. 2017. Lignin peroxidase functionalities and prospective applications. Microbiol Open. 6(1):e00394.

Fortea M, López-Miranda S, Serrano-Martínez A, Carreño J, Núñez-Delicado E. 2009. Kinetic characterisation and thermal inactivation study of polyphenol oxidase and peroxidase from table grape (*Crimson Seedless*). Food Chem. 113(4):1008–1014.

Fortea M, Lopez-Miranda S, Serrano-Martinez A, Hernandez-Sanchez P, Zafrilla M, Martinez-Cacha A, Nunez-Delicado E. 2011. Kinetic characterisation and thermal inactivation study of red alga (*Mastocarpus stellatus*) peroxidase. Food Chem. 127(3):1091–1096.

Freitas R, Paula R, Feitosa J, Rocha S, Sierakowski M-R. 2004. Amylose contents, rheological properties and gelatinization kinetics of yam (*Dioscorea alata*) and cassava (*Manihot utilissima*) starches. Carbohydr Polym. 55(1):3–8.

Gracas JP, Ranocha P, Vitorello VA, Savelli B, Jamet E, Dunand C, Burlat V. 2020. The Class III peroxidase encoding gene *AtPrx*62 positively and spatiotemporally regulates the low pH-induced cell death in *Arabidopsis thaliana* roots. IJMS. 21(19):7191.

Hamed RR, Maharem TM, Abel Fatah MM, Ataya FS. 1998. Purification of peroxidase isoenzymes from turnip roots. Phytochemistry. 48(8):1291–1294.

Hua H, Zhang W, Li J, Chang l, Li J, Guo Y, Cheng Y, Pi F, Xie Y, Yao W, et al. 2013. Purification and identification of antioxidant peptides from corn gluten meal. J Funct Foods. 5:1810–1821.

Jahangoshaei P, Hassani L, Mohammadi F, Hamidi A, Mohammadi K. 2015. Investigating the effect of gallium curcumin and gallium diacetylcurcumin complexes on the structure, function and oxidative stability of the peroxidase enzyme and their anticancer and antibacterial activities. J Biol Inorg Chem. 20(7):1135–1146.

Jaouadi B, Rekik H, Badis A, Jaouadi Zaraî N, Belhoul M, Hmidi M, Kourdali S, Fodil D, Bejar S. 2014. Production, purification, and characterization of a highly thermostable and humic acid biodegrading peroxidase from a decolorizing *Streptomyces albidoflavus* strain TN644 isolated from a Tunisian off-shore oil field. Int Biodeterior Biodegrad. 90: 36–44.

Kalin R, Atasever A, Ozdemir H. 2014. Single-step purification of peroxidase by 4-aminobenzohydrazide from Turkish blackradish and Turnip roots. Food Chem. 150:335–340.

Khanmohammadi M, Dastjerdi MB, Ai A, Ahmadi A, Godarzi A, Rahimi A, Ai J. 2018. Horseradish peroxidase-catalyzed hydrogelation for biomedical applications. Biomater Sci. 6(6):1286–1298.

Laemmli UK. 1970. Cleavage of structural proteins during the assembly of the head of bacteriophage T4. Nature. 227(5259):680–685.

Lataief S, Zourgui MN, Rahmani R, Najjaa H, Gharsallah N, Zourgui L. 2021. Chemical composition, antioxidant, antimicrobial and cytotoxic activities of bioactive compounds extracted from *Opuntia dillenii* cladodes. Food Measure. 15(1):782–794.

Lavery CB, Macinnis MC, Macdonald MJ, Williams JB, Spencer CA, Burke AA, Irwin DJG, D'Cunha GB. 2010. Purification of peroxidase from horseradish (*Armoracia rusticana*) roots. J Agric Food Chem. 58(15):8471–8476.

Li TS. 2008. Vegetables and fruits: nutritional and therapeutic values. Boca Raton, FL: CRC Press, p. 296.

Li Y, Jiang B, Zhang T, Mu W, Liu J. 2008. Antioxidant and free radical-scavenging activities of chickpea protein hydrolysate (CPH). Food Chem. 106(2):444–450.

Liu R, Xing L, Fu Q, Zhou GH, Zhang WG. 2016. A review of antioxidant peptides derived from meat muscle and by-products. Antioxidants. 5(3):32.

Liu X, Gao Y, Peng X, Yang B, Xu H, Zhao J. 2008. Inactivation of peroxidase and polyphenol oxidase in red beet (*Beta vulgaris* L.) extract with high pressure carbon dioxide. Innov Food Sci Emerg Technol. 9(1):24–31.

Lueangjaroenkit P, Kunitake E, Sakka M, Kimura T, Teerapatsakul C, Sakka K, Chitradon L. 2020. Light regulation of two new manganese peroxidase-encoding genes in *Trametes polyzona* KU-RNW027. Microorganisms. 8(6): 852.

Maciel HPF, Gouvêa CMCP, Toyama M, Smolka M, Marangoni S, Pastore GM. 2007. Extraction, purification and biochemical characterization of a peroxidase from *Copaifera langsdorffii* leaves. Quím Nova. 30(5):1067–1071.

Marzouki SM, Limam F, Smaali MI, Ulber R, Marzouki MN. 2005. A new thermostable peroxidase from garlic *Allium sativum*: purification, biochemical properties, immobilization, and use in H_2O_2 detection in milk. Appl Biochem Biotechnol. 127(3):201–214.

Mbadinga Mbadinga DL, Li Q, Ranocha P, Martinez Y, Dunand C. 2020. Global analysis of non-animal peroxidases provides insights into the evolution of this gene family in the green lineage. J Exp Bot. 71(11):3350–3360.

Mechri S, Sellem I, Bouacem K, Jabeur F, Chamkha M, Hacene H, Bouanane-Darenfed A, Jaouadi B. 2020a. Antioxidant and enzyme inhibitory activities of *Metapenaeus monoceros* by-product hydrolysates elaborated by purified alkaline proteases. Waste Biomass Valor. 11(12):6741–6755.

Mechri S, Sellem I, Bouacem K, Jabeur F, Laribi-Habchi H, Mellouli L, Hacène H, Bouanane-Darenfed A, Jaouadi B. 2020b. A biological clean processing approach for the valorization of speckled shrimp *Metapenaeus monoceros* by-product as a source of bioactive compounds. Environ Sci Pollut Res Int. 27(13):15842–15855.

Motamed S, Ghaemmaghami F, Alemzadeh I. 2009. Turnip (*Brassica rapa*) peroxidase: purification and characterization. Ind Eng Chem Res. 48(23):10614–10618.

Oztekin A, Almaz Z, Gerni S, Erel D, Kocak SM, Sengül ME, Ozdemir H. 2019. Purification of peroxidase enzyme from radish species in fast and high yield with affinity chromatography technique. J Chromatogr B Analyt Technol Biomed Life Sci. 1114–1115:86–92.

Papuc C, Goran GV, Predescu CN, Nicorescu V, Stefan G. 2017. Plant polyphenols as antioxidant and antibacterial agents for shelf-life extension of meat and meat products: classification, structures, sources, and action mechanisms. Compr Rev Food Sci Food Saf. 16(6):1243–1268.

Payet B, Shum Cheong Sing A, Smadja J. 2005. Assessment of antioxidant activity of cane brown sugars by ABTS and DPPH radical scavenging assays: determination of their polyphenolic and volatile constituents. J Agric Food Chem. 53(26):10074–10079.

Pech-Canul AC, Carrillo-Campos J, Ballinas-Casarrubias ML, Solis-Oviedo RL, Hernandez-Rascon SK, Hernandez-Ochoa LR, Gutierrez-Mendez N, Garcia-Triana A. 2020. Functional expression and one-step protein purification of manganese peroxidase 1 (rMnP1) from *Phanerochaete chrysosporium* using the *E. coli*-expression system. IJMS. 21(2):416.

Prat AG, Bolter C, Chavez U, Taylor C, Chefurka W, Turrens JF. 1991. Purification of cytochrome c peroxidase for monitoring H_2O_2 production. Free Radic Biol Med. 11(6): 537–544.

Qian Z-J, Jung W-K, Kim S-K. 2008. Free radical scavenging activity of a novel antioxidative peptide purified from hydrolysate of bullfrog skin, *Rana catesbeiana* Shaw. Bioresour Technol. 99(6):1690–1698.

Rajhans G, Sen SK, Barik A, Raut S. 2020. Elucidation of fungal dye-decolourizing peroxidase (DyP) and ligninolytic enzyme activities in decolourization and mineralization of azo dyes. J Appl Microbiol. 129(6):1633–1643.

Regalado C, Asenjo JA, Pyle DL. 1996. Studies on the purification of peroxidase from horseradish roots using reverse micelles. Enzyme Microb Technol. 18(5):332–339.

Rekik H, Zaraî Jaouadi N, Bouacem K, Zenati B, Kourdali S, Badis A, Annane R, Bouanane-Darenfed A, Bejar S, Jaouadi B. 2019. Physical and enzymatic properties of a new manganese peroxidase from the white-rot fungus *Trametes pubescens* strain i8 for lignin biodegradation and textile-dyes biodecolorization. Int J Biol Macromol. 125:514–525.

Rojas-Reyes JO, Robles-Olvera V, Carvajal-Zarrabal O, Castro Matinez C, Waliszewski KN, Aguilar-Uscanga MG. 2014. Purification and characterization of peroxidase from avocado (*Persea americana* Mill, cv. Hass). J Sci Food Agric. 94(9):1844–1853.

Rosa GP, Barreto MDC, Pinto D, Seca AML. 2020. A green and simple protocol for extraction and application of a peroxidase-rich enzymatic extract. Methods Protoc. 3(2): 25.

Sellem I, Kaaniche F, Chakchouk AM, Mellouli L. 2016. Antioxidant, antimicrobial and anti-acetylcholinesterase activities of organic extracts from aerial parts of three Tunisian plants and correlation with polyphenols and flavonoids contents. Bangladesh J Pharmacol. 11(2):531–544.

Serrano-Martínez A, Fortea M, Del Amor F, Núñez-Delicado E. 2008. Kinetic characterisation and thermal inactivation study of partially purified red pepper (*Capsicum annuum* L.) peroxidase. Food Chem. 107(1):193–199.

Simonetti E, Veronico P, Melillo MT, Delibes A, Andres MF, Lopez-Brana I. 2009. Analysis of class III peroxidase genes expressed in roots of resistant and susceptible wheat lines infected by *Heterodera avenae*. Mol Plant Microbe Interact. 22(9):1081–1092.

Singh N, Singh J. 2003. A method for large scale purification of turnip peroxidase and its characterization. Prep Biochem Biotechnol. 33(2):125–135.

Somtürk B, Kalı n R, Özdemir N. 2014. Purification of Peroxidase from Red Cabbage (*Brassica oleracea* var. *capitata f. rubra*) by affinity chromatography. Appl Biochem Biotechnol. 173(7):1815–1828.

Sumathi S, Pattabiraman T. 1977. Natural plant enzyme inhibitors V. A trypsin/chymotrypsin inhibitor from *Alocasia macrorhiza* tuber. Biochim Biophys Acta (BBA)-Enzymol. 485(1):167–178.

Thongsook T, Barrett DM. 2005. Purification and partial characterization of broccoli (*Brassica oleracea* var. *italica*) Peroxidases. J Agric Food Chem. 53(8):3206–3214.

Umeno A, Biju V, Yoshida Y. 2017. In vivo ROS production and use of oxidative stress-derived biomarkers to detect the onset of diseases such as Alzheimer's disease, Parkinson's disease, and diabetes. Free Radic Res. 51(4): 413–427.

Walwyn DR, Huddy SM, Rybicki EP. 2015. Techno-economic analysis of horseradish peroxidase production using a transient expression system in *Nicotiana benthamiana*. Appl Biochem Biotechnol. 175(2):841–854.

Wedelsbäck Bladh K, Olsson K. 2011. Introduction and use of horseradish (*Armoracia rusticana*) as food and medicine from antiquity to the present: emphasis on the Nordic countries. J Herbs Spices Med Plants. 17(3):197–213.

Wingfield P. 2001. Protein precipitation using ammonium sulfate. Curr Protoc Protein Sci. Appendix 3:Appendix 3F.

Xu G, Chance MR. 2007. Hydroxyl radical-mediated modification of proteins as probes for structural proteomics. Chem Rev. 107(8):3514–3543.

Yan J, Yuan SS, Jiang LL, Ye XJ, Ng TB, Wu ZJ. 2015. Plant antifungal proteins and their applications in agriculture. Appl Microbiol Biotechnol. 99(12):4961–4981.

Yang S, Yang J, Wang T, Li L, Yu S, Jia R, Chen P. 2020. Construction of a combined enzyme system of graphene oxide and manganese peroxidase for efficient oxidation of aromatic compounds. Nanoscale. 12(14):7976–7985.

Yen GC, Chen HY. 1995. Antioxidant activity of various tea extracts in relation to their antimutagenicity. J Agric Food Chem. 43(1):27–32.

Yumoto I, Ichihashi D, Iwata H, Istokovics A, Ichise N, Matsuyama H, Okuyama H, Kawasaki K. 2000. Purification and characterization of a catalase from the facultatively psychrophilic bacterium *Vibrio rumoiensis* S-1(T) exhibiting high catalase activity. J Bacteriol. 182(7):1903–1909.

Zeyadi M. 2019. Purification and characterization of peroxidase from date palm cv. Agwa fruits. Int J of Food Prop. 22(1):1910–1919.

Zhuang H, Tang N, Yuan Y. 2013. Purification and identification of antioxidant peptides from corn gluten meal. J Funct Foods. 5(4):1810–1821.

Zourgui M, Hfaiedh M, Brahmi D, Affi W, Gharsallah N, Zourgui L, Mohamed A. 2020. Phytochemical screening, antioxidant and antimicrobial activities of *Opuntia streptacantha* fruit skin. Food Measure. 14(5): 2721–2733.